Ecology Letters

WILEY

ECOLOGY LETTERS

LETTER

Choices to Landscapes: Mechanisms of Animal Movement Scale to Landscape Patterns of Space Use

Will Rogers[1] | Scott Yanco[1,2,3] | Walter Jetz[1,2]

[1]Department of Ecology & Evolutionary Biology, Yale University, New Haven, Connecticut, USA | [2]Center for Biodiversity and Global Change, Yale University, New Haven, Connecticut, USA | [3]Smithsonian's National Zoo and Conservation Biology Institute, Washington, DC, USA

Correspondence: Will Rogers (will.rogers@yale.edu; rogerswill47@gmail.com)

Received: 10 March 2025 | **Revised:** 27 October 2025 | **Accepted:** 17 November 2025

Editor: Jason Matthiopoulos

Keywords: ergodicity | habitat selection | movement | occurrence | resource selection | species distribution | step selection

ABSTRACT

Understanding animal space use is central to ecology and conservation, and movement-based habitat selection models provide powerful tools for identifying preferred environments. However, in heterogeneous landscapes, movement constraints limit habitat accessibility, decoupling realised space use from underlying preferences and complicating efforts to scale individual-level movement processes to landscape distributions. We present a steady-state distribution (SSD) framework that integrates locally estimated habitat selection and movement into sparse Markovian transition matrices to predict emergent space use. Across simulations and empirical case studies, SSD consistently outperformed occurrence-based models in predicting space use from individual- to population-level scales. Moreover, SSD proved to be more efficient—and sometimes even more accurate—than more assumptive agent-based model simulations (ABMs). Our approach bridges a key gap between mechanistic movement models and spatial prediction, providing a scalable and computationally efficient approach for translating individual movement behaviour into landscape-scale distribution patterns relevant for ecological inference and conservation planning.

1 | Introduction

Understanding the environmental limitations on organisms is central to explaining where they occur in space (James et al. 1984; Pulliam 2000; Soberón 2007). A core challenge in predicting species distributions is distinguishing between areas that are unsuitable and those that are suitable but inaccessible, given dispersal limitations or geographic barriers (Pulliam 2000; Soberón and Peterson 2005; Barve et al. 2011). Movement constraints ultimately shape access to suitable habitats, determining both local space use (Andrén 1994) and global distributions (Munguía et al. 2008). At individual scales, movement constraints can decouple observed space use from underlying habitat preferences (Schick et al. 2008; Matthiopoulos et al. 2020) (Figure 1). As GPS tracking datasets expand rapidly (Kays and Wikelski 2023; Davidson et al. 2025) with increasing calls to leverage movement data for biodiversity monitoring (Jetz et al. 2022), a critical challenge remains: how to scale individual-level habitat selection and movement processes to predict population- and species-level spatial distributions (Gomez et al. 2025).

Nevertheless, many models of animal distributions implicitly ignore movement constraints. For instance, species distribution models, occupancy models, and resource selection functions (RSFs) are frameworks under the umbrella of spatial point process models (Aarts et al. 2012), which correlate occurrence data with environmental attributes (Boyce and McDonald 1999; MacKenzie et al. 2006; Elith and Leathwick 2009; Elith et al. 2011; Merow et al. 2014). These occurrence-based models implicitly average over underlying ecological processes shaping species distributions.

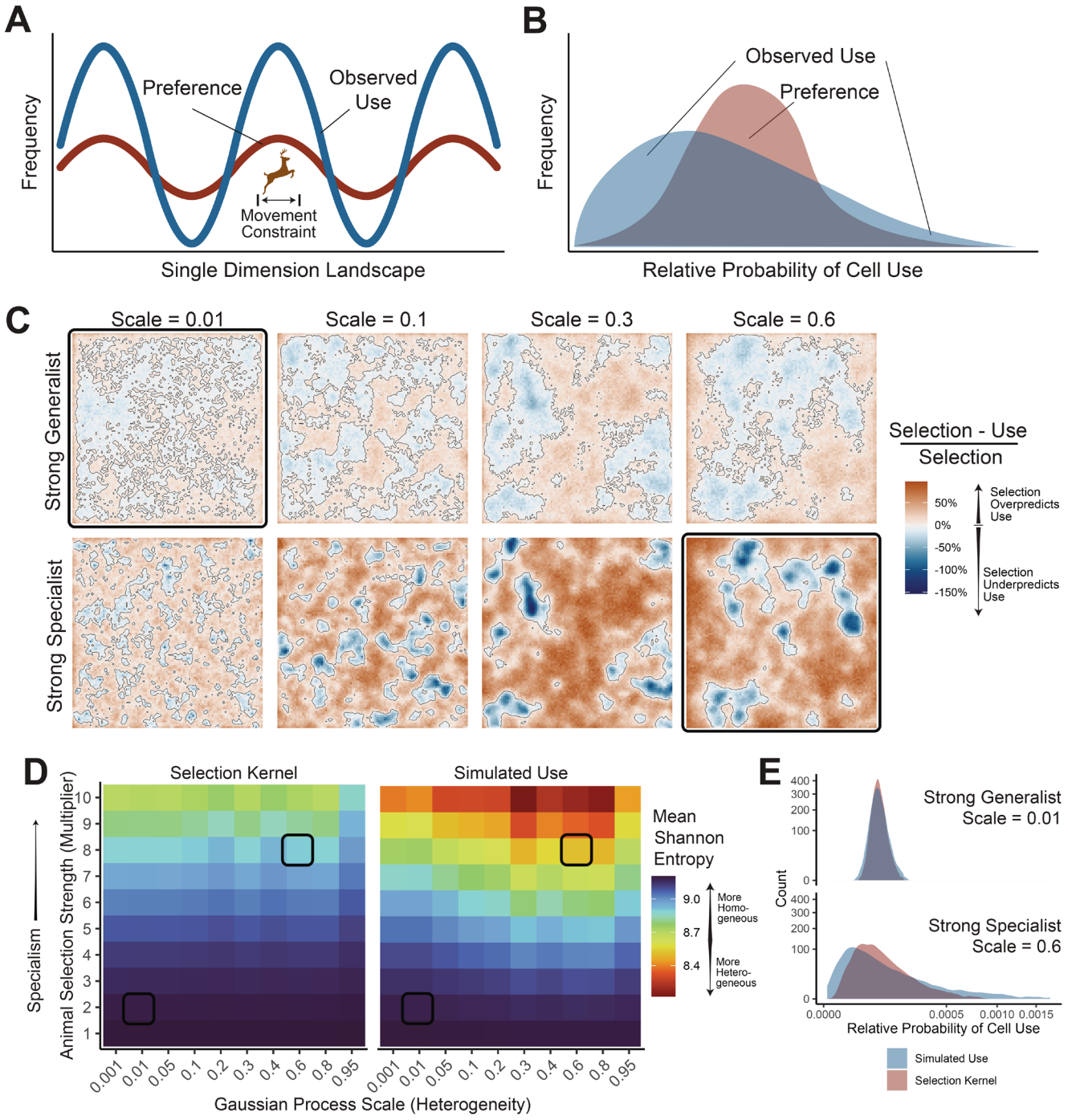

FIGURE 1 | Habitat preferences do not equal observed use in simulations. An organism's fundamental habitat preferences will not equal observed space use in heterogeneous landscapes where animals are movement-constrained, and this disparity may grow as habitat selection strength (or specialism) increases. (A) For example, expected space use in one dimension based solely on habitat preference (red) should diverge from actual use when movement constraints are imposed in a heterogeneous landscape (blue). (B) The corresponding spatial frequency distribution of cell use across the landscape without (red) and with (blue) movement constraints. (C) Simulated differences between habitat selection and actual space use under varying landscape heterogeneity (rows: Gaussian random field scale) and selection strength (columns: preference multiplier from 2 [generalist] to 8 [specialist]). Differences are shown as the proportional deviation of actual use from the selection kernel. Red indicates areas where the selection kernel overpredicts space use; blue indicates underprediction. Contour lines show transition zones. (D) Mean Shannon entropy (spatial evenness) of selection kernels versus actual use across simulations, comparing effects of selection strength (*y*-axis) and landscape heterogeneity (*x*-axis). (E) For two example scenarios (specialist in high heterogeneity; generalist in low heterogeneity, marked in C and D), density plots compare relative probabilities of use predicted by selection kernels (red) and actual use (blue). 'Strong Generalist' and 'Strong Specialist' map to animal selection strength multipliers 2 and 8, respectively.

For example, RSFs assume that all environmental conditions within a domain (e.g., home range) are equally accessible to animals, representing time-averaged habitat use as a function of environmental preference alone (Johnson et al. 2013). By conflating habitat selection with accessibility, occurrence-based models risk failure when generalising to new conditions

(Pearson and Dawson 2003). This problem is amplified in telemetry studies, where tracked individuals sample limited portions of available environments, making it difficult to treat GPS fixes as occurrence data and generalise across space or individuals (Nathan et al. 2008; Hooten et al. 2017; Alston et al. 2023).

Mechanistic movement models offer an alternative conceptual approach by explicitly modelling both habitat selection and movement constraints at fine spatial scales. Among them, integrated step-selection functions (iSSFs) are now widely used to infer habitat selection and movement behaviour (Avgar et al. 2016; Fieberg et al. 2021). iSSFs model stepwise habitat selection conditioned on locally available environments, concurrently estimating both habitat preferences and movement constraints. As a result, iSSFs offer a more mechanistically grounded alternative to occurrence-based models, potentially improving accuracy and generalisability. However, iSSF predictions are inherently local: naïve predictions from iSSF-derived habitat selection kernels fail to capture emergent space use patterns, especially in heterogeneous environments (Barnett and Moorcroft 2008; Avgar et al. 2016; Signer et al. 2017; Michelot et al. 2019). To address this, agent-based model simulations (ABMs) (Signer et al. 2017, 2024; Potts and Borger 2023; Forrest et al. 2024), Markov Chain Monte Carlo approaches (Michelot et al. 2019), partial differential equations (Barnett and Moorcroft 2008), or master equations (Potts et al. 2014) have been proposed to integrate local habitat selection and movement constraints to predict broader space use. However, these approaches (particularly ABM simulations) are often computationally intensive and may not converge (i.e., are non-ergodic). Alternative multi-stage frameworks that separately model habitat selection and movement constraints are more scalable but require treating movement and habitat selection as distinct processes (Van Moorter et al. 2023). Efficiently integrating habitat selection and movement constraints into spatial predictions remains an open challenge.

Here, we address this challenge by introducing a steady-state distribution (SSD) framework that converts iSSF-estimated local movement and selection processes into spatial predictions of animal space use. Building on connectivity modelling approaches (Fletcher Jr. et al. 2019), we represent movements as a Markov process, populate sparse transition matrices using iSSF-estimated movement probabilities, and solve for steady-state distributions. Leveraging the inherently local nature of animal movement simplifies transition matrices, drastically reducing computational costs with minimal-to-no loss in accuracy. We evaluated SSD performance relative to RSF, naïve SSF, and ABM predictions using (i) simulations across gradients of habitat heterogeneity and selection strength and (ii) empirical case studies spanning multiple species and spatial scales. Our findings demonstrate that SSD offers scalable, mechanistically grounded predictions of animal space use, linking individual movement behaviour to population-scale spatial distributions.

2 | Methods

We developed and evaluated a framework to estimate population-level space use from individual-level iSSF movement models, combining empirical selection patterns and movement constraints in a single framework. We describe the basis of this approach and then detail the simulations and empirical systems used to evaluate our framework.

2.1 | Landscapes as Transition Matrices

Motivated by approaches in connectivity modelling (McRae et al. 2008; Fletcher Jr. et al. 2019), we define a landscape, G, composed of n discrete cells, each representing a location and associated environmental data (Figure 2A). We represent animal movement between cells as a Markov process in a row-stochastic transition matrix, A, wherein each element $A_{i,j}$ reflects the probability of moving from one cell, G_i, to another, G_j. We use eigendecomposition to find the expected proportion of time an animal spends in each cell or stable state distribution (π), which is the dominant left eigenvector of A satisfying $\pi^T A = \pi^T$, analogous to stable stage distributions in Leslie matrices (Leslie 1945).

The spatial domain of G imposes a hard boundary: transition probabilities are only defined within G, effectively preventing unbounded diffusion. As a result, SSD predictions are conditional on the chosen spatial domain. The extent and resolution of G should therefore align with the ecological scale of interest (e.g., home ranges, population distributions), and SSD predictions should always be interpreted relative to the defined domain.

2.2 | Parameterising Transition Matrices With iSSFs

We parameterised the transition probabilities in A using fitted iSSFs. Starting in G_i, the sum of all transition probabilities to all other cells in G (including remaining in G_i) must sum to one:

$$\sum_{k=1,}^{n} A_{i,k} = \sum_{k=1,}^{n} P\left(G_k \middle| G_i\right) = 1. \quad (1)$$

iSSF models include two components—a movement kernel and a selection function for a set of environmental variables (Avgar et al. 2016; Fieberg et al. 2021). Estimates of selection based on iSSFs are therefore always conditional upon a baseline set of environmental and movement covariates, and differences in predictions relative to this baseline set of conditions (or relative risk) are often described as relative selection strength (RSS) (Avgar et al. 2017). For example, we used iSSFs to estimate the RSS for a candidate location (G_j) by comparing it against an alternative set of conditions (G_i), defined as:

$$RSS\left(G_j \middle| G_i\right) = \frac{e^{\left(\beta_1 h(G_j) + \beta_2 m(G_i, G_j)\right)}}{e^{\left(\beta_1 h(G_i) + \beta_2 m(G_i, G_i)\right)}}, \quad (2)$$

where β_1 is a vector of habitat selection coefficients associated with a matrix, h, of environmental conditions at sites G_i and G_j, and β_2 is a vector of movement selection coefficients associated with a matrix, m, of step lengths between cells. Turn angles between movements were not included because they break Markovian assumptions.

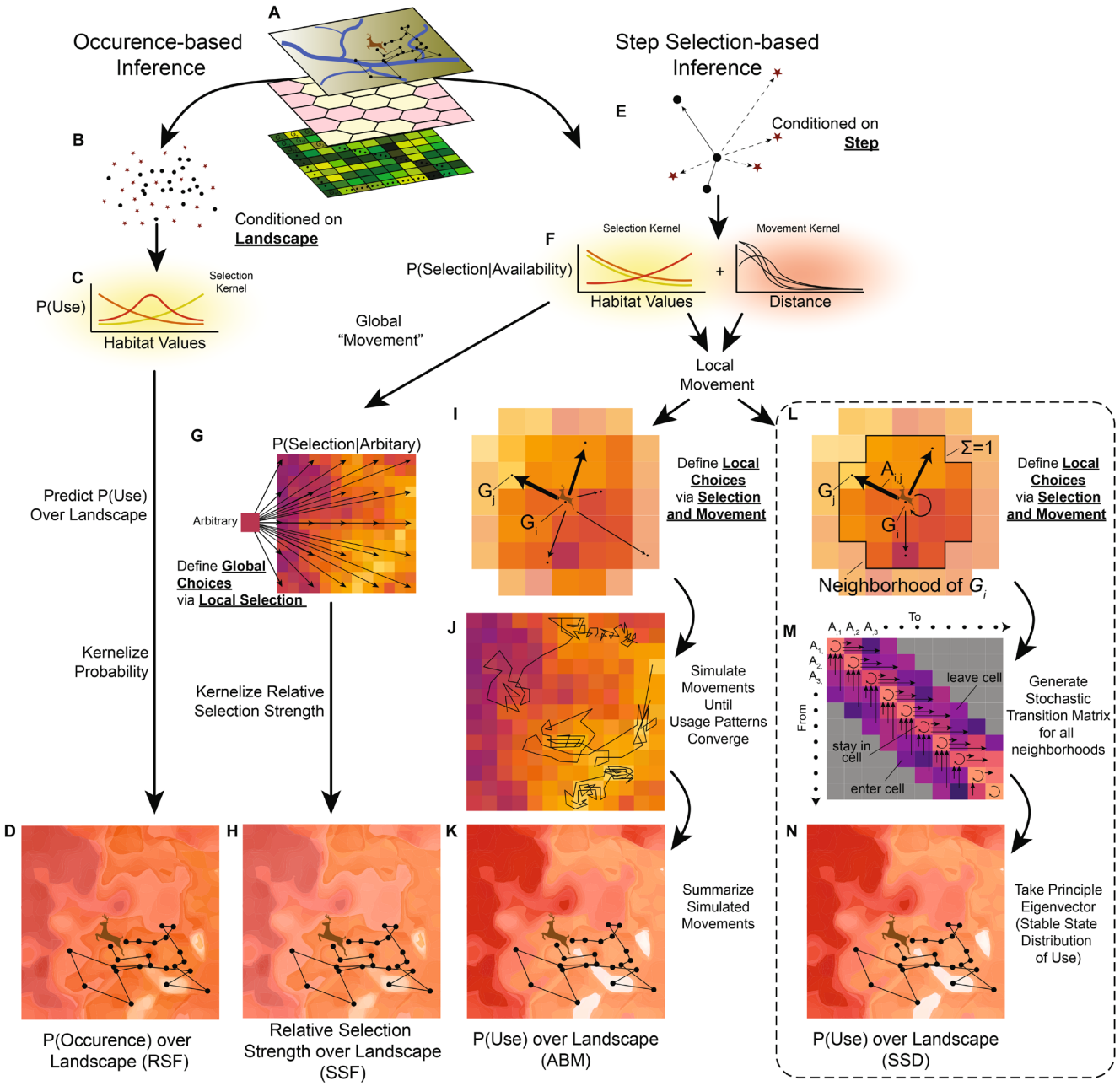

FIGURE 2 | Movement data-based landscape predictions. Converting animal movements into spatial predictions of use can occur in four main ways. (A) Animal movements are observed within a landscape composed of discrete cells where each location can be linked to environmental attributes. (B) Animal locations can then be placed into use versus available frameworks conditional on the landscape in resource selection analyses (RSFs), where (C) RSFs predict the probability of use over a landscape, but are unable to separate the role of habitat selection or movement in shaping occurrence. (D) Resulting RSF predictions can be kernelised to return probabilities of use over *G*. (E) Alternatively, tracking data can be converted into use versus available frameworks conditional on steps for integrated step-selection analyses (iSSFs). (F) iSSFs explicitly separate habitat selection from movement, estimating the relative risk of taking a step based on local environmental and movement contexts—termed relative selection strength. (G) Naïve SSF predictions project relative selection strengths across *G*, given arbitrary starting conditions, and (H) relative selection strengths can be kernelised, representing something visually akin to RSF output, though mathematically inequivalent. (I) In contrast, agent-based models (ABMs) simulate individual movements directly, using empirically derived step lengths, turn angles, and environmental selection to generate local movement probabilities. (J) By iterating this process millions of times, (K) we can approximate the long-term probability of space use. (L) Similar to ABMs, we can use iSSFs to estimate the probability of movement within local 'neighbourhoods' defined by movement constraints. (M) We can aggregate probabilities of entering, leaving, or staying in cells into a sparse stochastic matrix. (N) Solving for the principal eigenvector of the stochastic matrix returns the stable state distribution of space use, given all possible starting points and infinitely many movements.

Importantly, RSS does not represent absolute movement probabilities but rather relative rates of movement (Avgar et al. 2016). To translate RSS into transition probabilities, we kernelised RSS estimates over the set of movements available from G_i to generate transition rates of remaining in or leaving G_i. For example, the probability of moving from G_i to G_j was:

$$A_{i,j} = P(G_j|G_i) = \frac{RSS(G_j|G_i)}{\sum_{l=1}^{n} RSS(G_l|G_i)}. \quad (3)$$

By kernelising RSS, we translated iSSF-derived RSS into transition probabilities $A_{i,j}$, directly linking local habitat selection and movement constraints to the transition matrix A. We used cell centroid conditions in G to define local transition matrices, assuming that variation within landscape cells is well described by average cell conditions or distance between cell centroids. To ensure predictions were defined when remaining in place, we forced zero step lengths to a very small value (0.001, orders of magnitude smaller than between-cell distances).

2.3 | Solving Computational Constraints With Movement Constraints

There are two main challenges in generating steady-state distribution (SSD) predictions using eigendecomposition. First, estimating transition probabilities between all cells based on fitted integrated step-selection functions (iSSFs) is computationally intensive, since there are n^2 possible transitions between n cells. Second, eigendecomposition of large transition matrices requires substantial RAM, proportional to the number of matrix elements.

To address these challenges, we leveraged the movement constraints in the original tracking data. iSSF movement kernels inherently down-weight selection for distant locations, even when those habitats are suitable (Avgar et al. 2016). Given this, we assumed that animal movement is generally limited to locally accessible habitat (neighbourhoods) defined by typical movement ranges (Figure 2L), and we represented A as sparse, only estimating $A_{i,j}$ for cell pairs within neighbourhoods (Figure 2M).

In practice, we used the 95th percentile of observed step lengths to define the radius of neighbourhoods. To defend this, we evaluated the effect of various neighbourhood sizes on SSD inferences, finding that increasing matrix sparsity provided large computational savings without reducing accuracy (details in Supporting Information S1). Although the impact of sparsity may vary depending on system-specific movement constraints and habitat heterogeneity, overall computational demands can be reduced by altering the resolution of G and by reducing neighbourhood sizes to make A sparser. For example, on a computer with 16 GB of RAM, we could solve SSDs for a matrix with over 324 million non-zero elements—equivalent to a landscape with 18,000 fully connected cells, or about 65 million cells if transitions are restricted to the four nearest neighbours. To further increase computational efficiency, we only solved for the first eigenvector using the package 'RSpectra' (Qiu and Jiali 2024) to access Spectra C++ libraries.

2.4 | Competing Prediction Types

We generated three alternative spatial predictions from movement data to compare against SSD. First, we produced occurrence-based RSFs, which contrast observed locations to available sites within an animal's home range ('RSF', Figure 2B–D). Second, we created naïve predictions based solely on iSSF habitat selection kernels and excluding movement constraints ('naïve SSF', Figure 2G,H), known to be poor predictors of utilisation distributions (Barnett and Moorcroft 2008; Avgar et al. 2016; Signer et al. 2017; Michelot et al. 2019). Third, we ran ABM simulations from full iSSF models, which included additional terms for turn angles omitted in the SSD approach ('ABM', Figure 2I–K). ABMs can be considered a gold standard because they explicitly simulate fine-scale movement processes. Though they should theoretically yield the most accurate predictions, ABMs are computationally intensive and may not converge to a stable distribution. This non-ergodicity arises because landscapes are complex with many possible initialisations, and the difficulty of achieving convergence increases with the size of G.

2.5 | Simulations

Both landscape heterogeneity and animal behaviour (e.g., habitat preferences) influence spatial distributions and may affect the performance of mechanistic movement models and predictive frameworks. To assess how these factors shape the accuracy of SSD, RSF, naïve SSF, and ABM predictions, we simulated animal movement data using the iSSF-based approach described by Potts and Borger (2023). Specifically, we generated four random environmental layers (100×100 cells) using Gaussian random fields with 10 levels of spatial autocorrelation (Hanson et al. 2024) (S1 Figures S1 and S2). On each landscape, we simulated animals exhibiting 10 different strengths of habitat selection for environmental variables (β_{1-4}, S1 Table S1), reflecting a gradient from generalist to specialist habitat selection. Simulated movements included an exponential decay in selection for longer step lengths and turn angles away from zero (i.e., preference for shorter steps and directional persistence). We generated 10,000 steps for modelling (S1 Figure S4) and 5 million steps per scenario for validation (Figure 1C–E). We replicated each combination of landscape heterogeneity and selection strength five times.

We then generated SSD, RSF, naïve SSF, and ABM space use predictions using simulated movements. For iSSFs, we sampled 100 random locations per step from a uniform distribution (0%–125% of the maximum observed step length) and fit models including environmental layers, step length, and log-step length as predictors (S1 Table S2) using 'amt' (Signer et al. 2019). We included step length and log-step length to force an exponential decay in selection for further steps (Avgar et al. 2016). We then generated SSD predictions based on fitted iSSFs. We fit RSFs by sampling 10 random points per used location within minimum convex polygons around use locations (to capture within home range selection), including environmental layers as predictors (S1 Table S2) using 'amt' (Signer et al. 2019). We generated naïve selection-only SSF predictions using fitted iSSFs to predict the RSS for all cells in the landscape. For ABMs, we refit iSSFs with an additional term for the cosine of turn angles (S1 Table S2). We then used the simulation framework from Signer et al. (2024) to simulate 5000 steps (sampling 100 possible movements per step) and discarded the initial 100 steps to avoid the influence of start conditions. We repeated this process 5000 times for a total of 2.45 million ABM locations per simulation.

We used Shannon entropy to measure the heterogeneity in spatial predictions, Bhattacharyya affinity to compare predictions to observed space use, and estimates of minimum core area (50% of total predicted use) to compare prediction types across levels of landscape heterogeneity and animal selection strength. We provide further description of the simulations in Supporting Information S1.

2.6 | Case Studies

We then evaluated SSD versus RSF, naïve SSF, and ABM using four animal movement datasets: (i) red deer (*Cervus elaphus*) in Northern Germany ($n = 1$) (Signer et al. 2019); (ii) roe deer (*Capreolus capreolus*) in Northern Italy ($n = 5$) (Cagnacci et al. 2011); (iii) fisher (*Pekania pennanti*) in Northern New York, USA ($n = 8$) (LaPoint et al. 2013); and (iv) African buffalo (*Syncerus caffer*) in Kruger National Park, South Africa ($n = 6$) (Cross et al. 2016). We modelled habitat selection using system-specific environmental covariates (S2 Tables S1 and S2). For the red deer dataset, we used distance to forest and forest cover, aggregated at 125 m × 125 m resolution across a 19 × 18 km landscape (S2 Figures S1–S5). For roe deer, we used open landcover, distance to forest, and slope at 100 m × 100 m resolution over a 12 × 14 km area (S2 Figures S6–S11). For fisher, we used distance to forest at 91 m × 123 m resolution over a 20 × 24 km (S2 Figures S12–S23). For buffalo, we used woody cover (Urban et al. 2020) and distance to water sources at 493 m × 493 m resolution across a 119 × 354 km landscape (S2 Figures S24–S30). To standardise within systems, we resampled movement data to a consistent GPS fix interval: red deer—6 h, roe deer—4 h, fisher—30 min, and buffalo—5 h. For roe deer, summer movements (Julian days 120–290) were analysed to exclude migratory behaviour.

For each GPS track, we used the first 75% of movement data (chronologically) as in-sample training data to fit individual-level habitat selection models using 'amt' (Signer et al. 2019). We generated RSF and iSSF models following the same use-availability designs as in simulations, including the system-specific environmental variables (S2 Table S2). For ABMs, we refit iSSFs with an additional term for the cosine of turn angles, and we used 100,000 simulated tracks of 5000 steps each (sampling 100 possible movements per step), removing the first 100 steps to limit the effect of random start locations. We visually assessed ABM convergence by calculating the Bhattacharyya affinity between subsampled sets of ABM tracks and the full simulation prediction surface (S2 Figures S34–S36).

We compared space use predictions from SSD, RSF, naïve SSF, and ABM predictions in two ways: (i) based on core area estimates and (ii) based on their ability to predict animal space use. To quantify core area, we calculated the minimum area containing 50% of total predicted use. To assess predictive performance, we evaluated model fit at four increasingly, out-of-sample scales: *In-Sample*—the 75% of movement data included in model fitting; *Within Individual*—the withheld 25% of an individual's data chronologically; *Between Individuals*—the tracking data of all other individuals in the same environmental context; and, *Between Contexts*—the tracking data of individuals in different environmental contexts. We defined *Between Contexts* based on spatial separation and differences in environmental attributes between tracked individuals (only relevant to fisher and buffalo). One fisher was located 30 km away from other tracked individuals in a landscape with less human infrastructure and larger forest patches (S2 Figures S12 and S13). Tracked buffalo were from two different herds, separated by 71 km with differences in distance to water, tree cover, and productivity (S2 Figures S24 and S25).

Validation datasets based on GPS tracking represent only a subset of an individual's total space use. Consequently, they are not well-suited for direct comparison to predicted probability distributions (e.g., using Bhattacharyya affinity) unless additional modelling steps are used to approximate unobserved space use. Instead, we used two evaluation metrics that do not rely on complete space use data: (i) the geometric mean of predicted use at observed locations, and (ii) the Spearman rank correlation between binned predicted use and observed use intensity across equal-area spatial bins (Boyce et al. 2002). Simulations showed that Spearman rank correlations can be biased toward selecting overly homogeneous prediction surfaces (see Supporting Information S1, S1 Figure S30). In contrast, the geometric mean more reliably distinguished model performance and tended to be more conservative (S1 Figure S31). Therefore, we emphasise geometric mean results in the main text, while reporting Spearman rank correlations in Supporting Information S2. Inferences were generally consistent across both metrics. To isolate model comparisons, we calculated pairwise differences between SSD predictions and those from RSF, naïve SSF, and ABM models. To assess the sensitivity of these comparisons to sampling variation, we bootstrapped validation datasets by resampling observed GPS points (with replacement) 100 times. Due to the computational cost of ABM simulations, we did not perform cross-validations that required resampling training data.

2.7 | African Buffalo Independent Population Density Comparison

As an additional validation, we compared SSD predictions to independent spatial buffalo census data collected by Kruger National Park. We used 29 years of helicopter counts of mixed-herd buffalo conducted between 1985 and 2012 and in 2017 (see Hughes et al. 2017; Staver et al. 2019). We compared whether the individual-level prediction surfaces (SSD, RSF, naïve SSF, and ABM) estimated from tracking data were correlated with buffalo abundance at census locations. We fit four mixed-effect negative binomial models with 'glmmTMB' (Brooks et al. 2017), using individual-level SSD, RSF, naïve SSF, or ABM predictions at specific census locations (scaled for model estimation) to predict census abundances. Within models, we accounted for individual-level (to address prediction differences across individuals) and annual random effects to account for demographic changes. We assessed model fit using 'DHARMa' (Hartig 2018) (S2 Figure S38), and we compared model performance using AIC scores (Akaike 1998).

2.8 | Supplements and Code

Further description of the method and simulations (Supporting Information S1) and empirical examples (Supporting

Information S2) are provided as supplements. Code and data to replicate the results are provided at https://github.com/will-rogers/SSD_Paper_Code and archived with Zenodo: https://doi.org/10.5281/zenodo.16794098 (Rogers et al. 2025).

3 | Results

Across both simulations and four empirical case studies, SSD predictions consistently outperformed both occurrence-based RSFs and naïve SSF-based predictions, and SSD matched or exceeded the accuracy of more computationally intensive ABM simulations. SSDs reliably captured the effects of habitat heterogeneity and selection strength on emergent space use, offering both predictive accuracy and computational efficiency. In empirical applications, SSDs further demonstrated strong generalisability, better scaling individual-level movement data to population-level space use.

3.1 | Simulation

As expected, we found strong mismatches between habitat preferences and emergent space use, particularly under strong habitat selection and high landscape heterogeneity (Figure 1C). Movement constraints concentrated space use, producing distributions that were substantially more restricted than expected from habitat preferences alone (Figure 1D,E). These effects also translated to habitat selection inferences: occurrence-based RSF estimates were highly sensitive to landscape structure and selection strength, while iSSF inferences were generally more stable (Figure 3B, S1 Figure S18).

Simulated space use patterns were most closely matched by SSD and ABM predictions (Figure 3E–G, S1 Figures S24–S26). SSD slightly outperformed ABMs in homogeneous landscapes and at lower selection strengths, while ABMs performed marginally better in highly heterogeneous environments (Figure 3E). In contrast, naïve SSF predictions consistently performed worst (Figure 3E), in line with previous work (Barnett and Moorcroft 2008; Avgar et al. 2016; Signer et al. 2017; Michelot et al. 2019). Interestingly, RSFs, though averaging over selection and movement mechanisms, generally outperformed naïve SSF predictions but remained substantially less accurate than SSD or ABMs (Figure 3E). Both RSF and naïve SSF approaches consistently overestimated core space use, often by more than 100% in complex landscapes or under strong selection (Figure 3F).

While both SSD and ABMs captured more accurate emergent space use patterns, SSD predictions more closely matched observed core areas (Figure 3F). Notably, SSD achieved this performance while requiring substantially less computational effort than ABMs. Individual ABM tracks converged slowly (Figure 3C,D, S1 Figures S15–S17), and tens of thousands of simulations were needed to approximate stable space use distributions (Figure 3C insets). By contrast, SSD produced comparable or better predictions in most simulation conditions. In total, these results demonstrate that SSD offers an efficient, mechanistically grounded alternative to ABMs for predicting emergent space use from local selection and movement processes. We also highlight that RSF and naïve SSF predictions are relatively poor proxies of space use, particularly in heterogeneous landscapes and strong habitat selection.

3.2 | Case Studies

In empirical case studies (red deer, roe deer, fisher, and African buffalo), SSD consistently generalised individual-level movement processes to out-of-sample and population-level space use more accurately than RSF, naïve SSF, or even ABM predictions (Figure 4). Based on predictive accuracy (geometric mean of predicted use at observed locations), SSD outperformed RSF in 78% of cases, naïve SSF in 64% of cases, and ABM in 59% of cases. Notably, the relative performance gain of SSD tended to increase under more challenging validation contexts, like predicting space use in the future, for other individuals, and in different environmental contexts. Both SSD and ABM predictions consistently produced more spatially concentrated core space use estimates than RSF or naïve SSF predictions (Figures 5D and 6B). Specifically, SSD predictions estimated approximately 20%–50% less core space use than RSF (except for buffalo) or naïve SSF and approximately 5%–50% less core habitat than ABM approaches, possibly because ABM movement kernels capture rarer long-distance movements (Figure 5D, S2 Figures S32 and S33).

As in simulations, ABMs required substantial computational effort to produce stable space use predictions, with convergence rates scaling with landscape size (S2 Figures S34–S36). Each ABM simulation track (5000 steps) took approximately 1.5 min to complete on a high-performance cluster, and approximately 10,000 tracks per individual were needed for predictions to stabilise (S2 Figures S34 and S35). This resulted in > 10 days of total computational time per prediction, though massively parallel processing could reduce this to ~2–3 h per individual. In contrast, SSD predictions were run locally on a 16 GB RAM laptop and took < 2.5 min per individual, guaranteed long-term space use convergence (ergodicity), and often outperformed ABM predictions. Together, these results demonstrate that SSD offers a scalable and computationally efficient alternative to ABMs, with better or comparable predictive performance across diverse empirical systems.

3.3 | Independent Population Density Comparison

Using GPS tracking from six individuals and 29 years of dry-season African buffalo census data from Kruger National Park (3751 herd detections, Figure 6A), we found that SSD predictions best explained spatial variation in population-level densities in a 19,300 km^2 ecosystem (Figure 6B,C, S2 Figure S24, S2 Table S3). While observed abundances correlated with both variation in naïve SSF (negative binomial generalised linear mixed-effect model [GLMM]: $\beta = 0.069$, standard error [SE] = 0.007, $p < 0.001$) and ABM prediction surfaces (negative binomial GLMM: $\beta = 0.030$, SE = 0.007, $p < 0.001$), there was a stronger relationship between the SSD surface and observed counts (negative binomial GLMM: $\beta = 0.091$, SE = 0.007, $p < 0.001$). Conversely, there was no relationship between RSF predictions and abundance (negative binomial GLMM: $\beta = -0.009$, SE = 0.007, $p = 0.169$). These results demonstrate that SSD approaches using individual-level movement data can scale up to predict long-term population

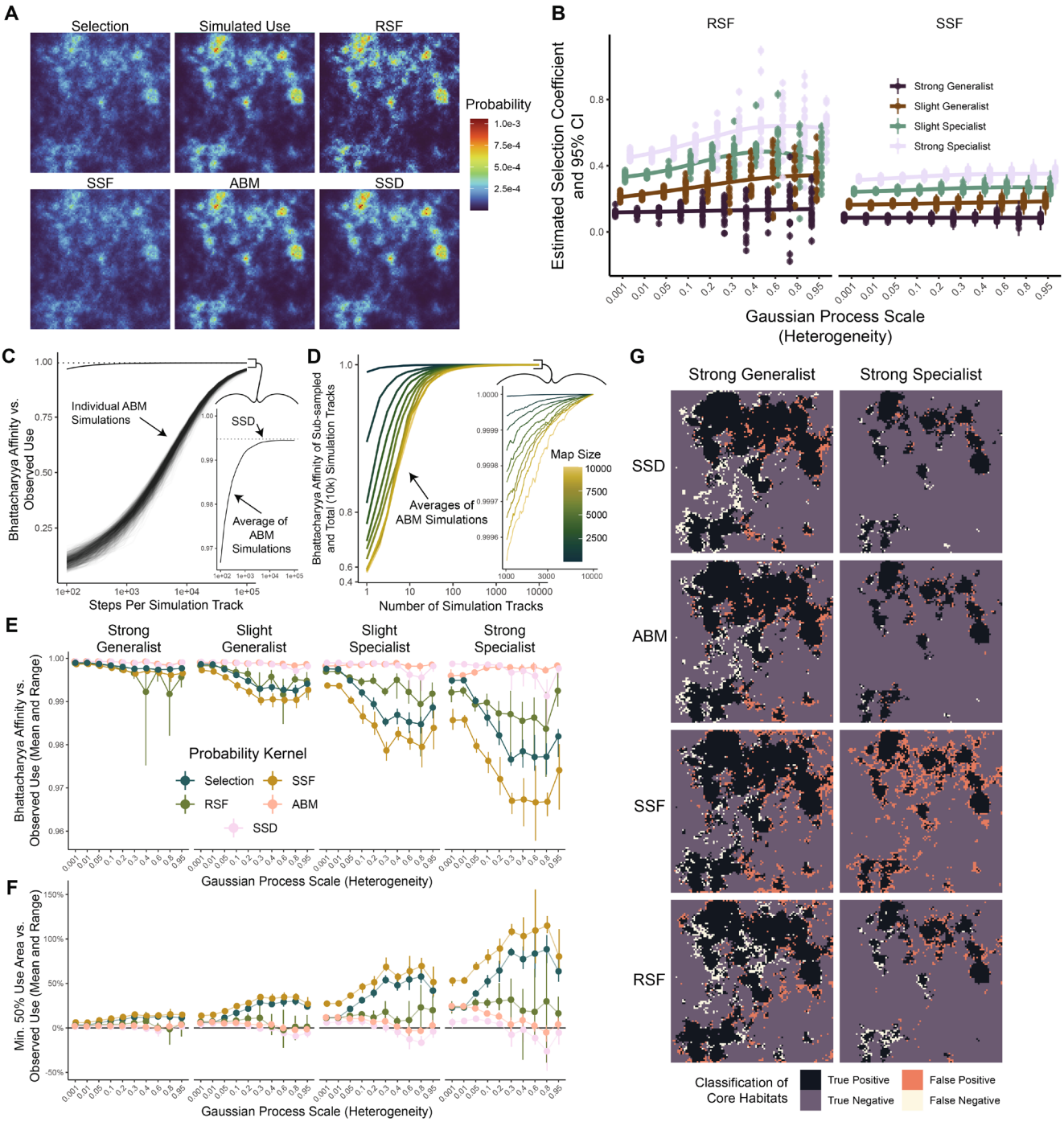

FIGURE 3 | Predictions incorporating movement mechanisms recover simulated patterns of use. (A) An example of simulation inputs, outputs, and predictions. We generated maps of underlying habitat selection and used these maps to simulate space use in 5 million steps with constraints on step length and turn angle. We also used a set of 10,000 steps to generate predictions from resource selection functions (RSFs), naïve step-selection functions (SSFs), agent-based model simulations (ABMs), and stable state distributions (SSDs). (B) Across five simulation sets varying in landscape heterogeneity (*x*-axis, Gaussian random field scale) and selection strength (colour scale), RSF estimates showed increasing variability under high heterogeneity and strong selection, whereas iSSF estimates remained more stable. We converted estimates and 95% confidence intervals (CIs) such that directions of true positive and negative selection coefficients are aligned (e.g., positive values imply more extreme inferences). (C) For ABMs, individual simulated tracks (shaded lines) converged slowly, if at all, toward observed space use based on Bhattacharyya affinity and (Inset) only after aggregating thousands of ABM runs (solid line) did predictions approximate SSD performance (dotted line). (D) ABM convergence rates were strongly influenced by landscape size (line colour) and (Inset) even after thousands of iterations, ABMs remained weakly converged, as indicated by Bhattacharyya affinity scores. (E) We compared SSD, RSF, SSF, and ABM predictions against simulated space use using Bhattacharyya affinity and (F) minimum core 50% use area across levels of landscape heterogeneity (*x*-axis) and selection strength (horizontal facets). (G) Finally, SSD, SSF, RSF, and ABM produced distinct spatial predictions of space use, illustrated by classifying habitats into top 50% use areas relative to simulated truth, across prediction methods (vertical facets), and selection strength levels (horizontal facets). 'Strong Generalist', 'Slight Generalist', 'Slight Specialist', and 'Strong Specialist' map to animal selection strength multipliers 2, 4, 6, and 8, respectfully.

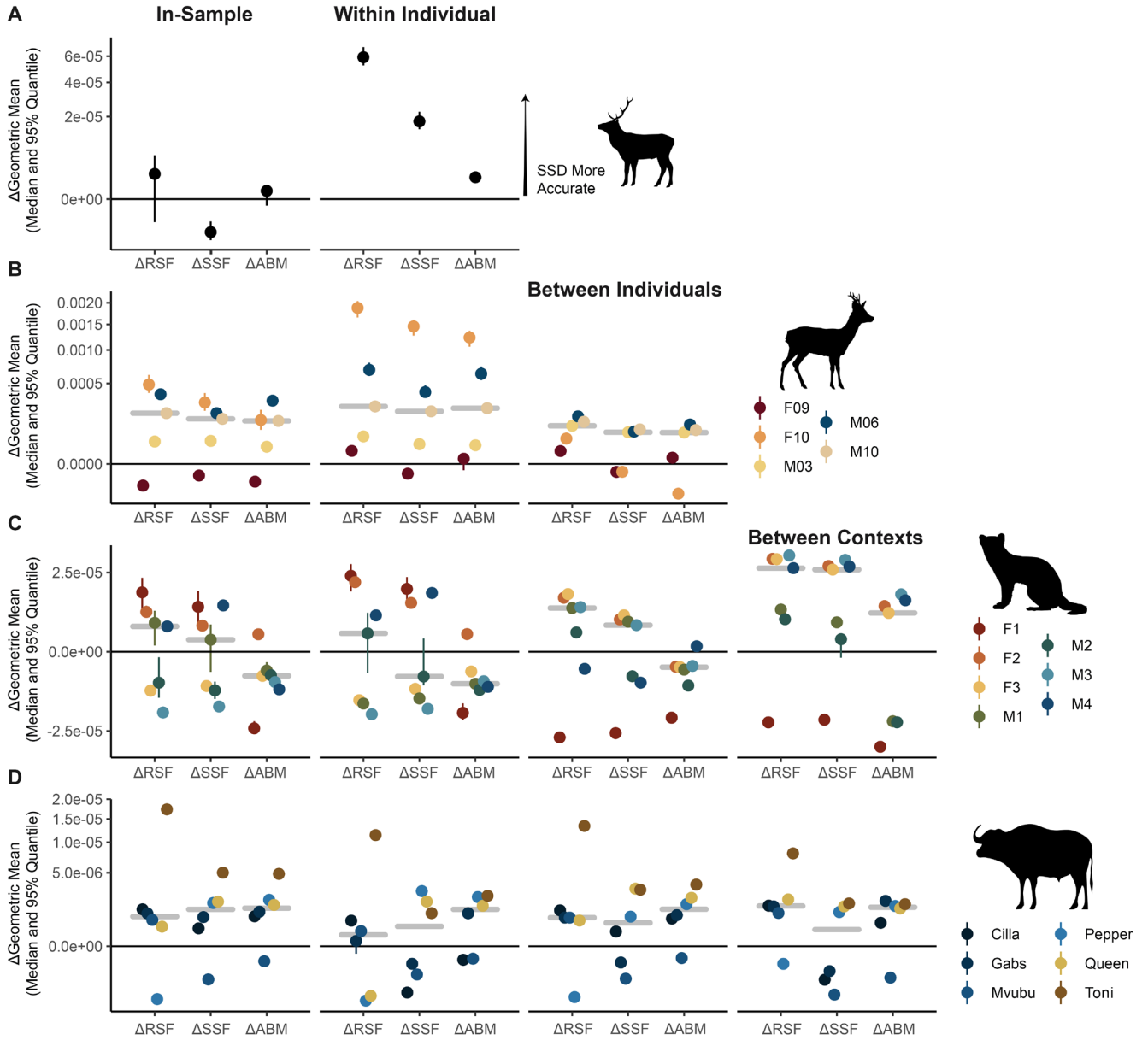

FIGURE 4 | Predictions incorporating movement mechanisms better predict out-of-sample animal movements. (A–D) Median and 95% quantiles in 100 bootstraps of pairwise differences between stable state distribution (SSD) and resource selection function (RSF), naïve step-selection function (SSF), or agent-based model (ABM) simulation predictions in the geometric mean of predicted probability of use at observed use sites. Bootstraps were performed by resampling modelled and out-of-sample data with replacement for (A) red deer, (B) roe deer, (C) fisher, and (D) African buffalo datasets. Validations were performed in four sets of comparisons: *In-Sample*—the first (chronologically) 75% of observed locations for individuals used in models; *Within Individual*—the next (chronologically) 25% of observed locations per individual withheld from models; *Between Individuals*—all observed locations for other individuals in a dataset in the same geographic context; and, *Between Contexts*—all observed locations for other individuals in a different environmental context than the individual modelled. For visualisation, the median difference for each set of comparisons is highlighted by a horizontal grey bar. All organism silhouettes are from PhyloPic (www.phylopic.org).

abundance across large ecosystems, surpassing occurrence-based RSFs, naïve SSFs, and ABM simulations.

4 | Discussion

Our results establish SSD as a scalable framework for predicting animal space use from movement mechanisms. By converting locally estimated habitat selection and movement constraints from iSSFs into Markovian transition matrices, SSD generates spatial predictions that integrate both habitat preferences and accessibility constraints. This is important because movement constraints can strongly shape habitat accessibility and resulting animal spatial distributions (Pulliam 2000; Soberón and Peterson 2005; Schick et al. 2008; Matthiopoulos et al. 2020; Van Moorter et al. 2023). Our simulations underscore how movement constraints produce sharp mismatches between habitat preferences and realised space use, especially in heterogeneous landscapes or under strong habitat selection. Occurrence-based RSFs, which implicitly average over habitat selection and accessibility, were poor predictors of space use in both simulations and case studies and generalised poorly to

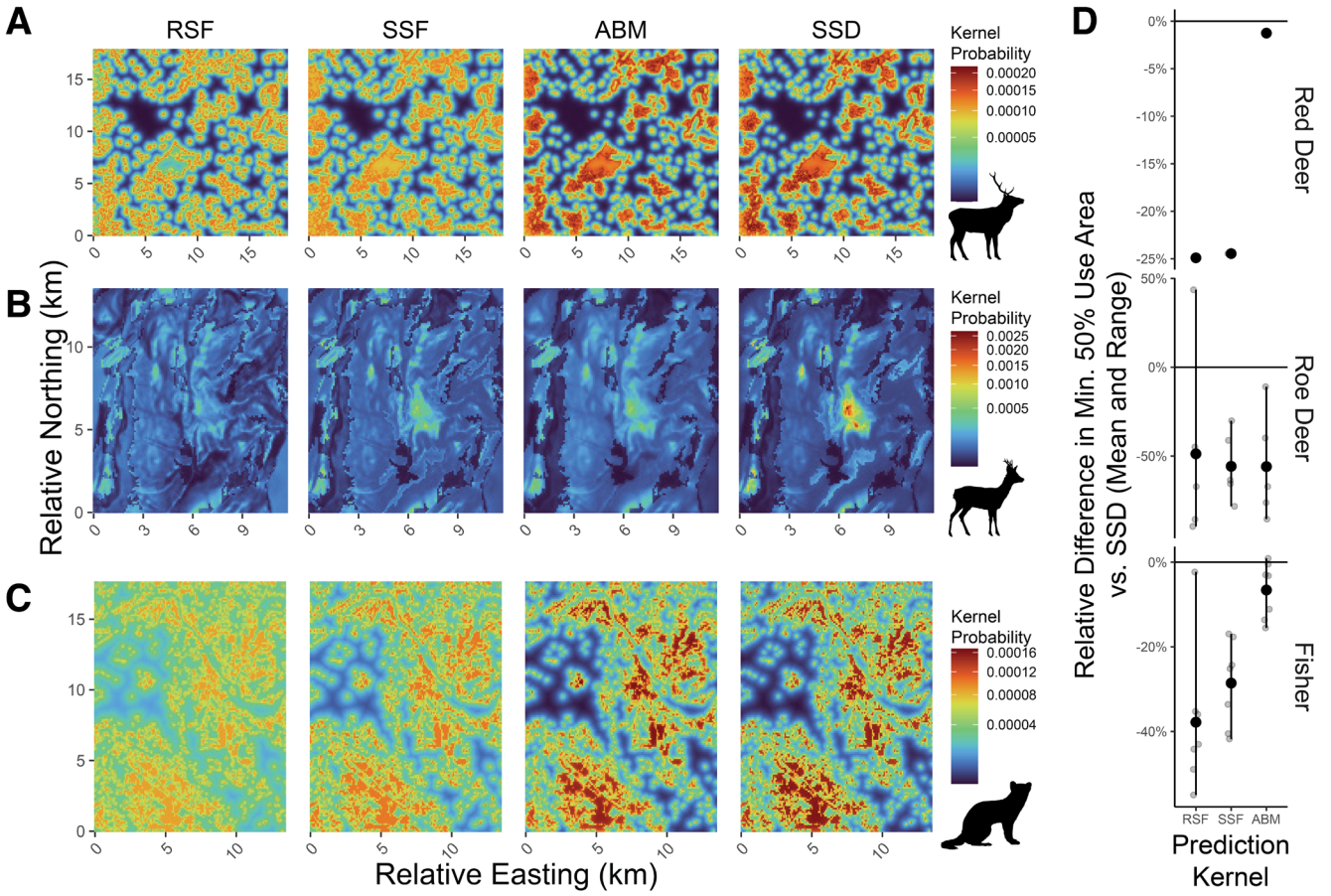

FIGURE 5 | Predictions incorporating movement mechanisms are more spatially concentrated than those based on selection alone. Stable state distribution (SSD), resource selection function (RSF), naïve step-selection function (SSF), and agent-based model simulation (ABM) average space use predictions for (A) red deer, (B) roe deer, (C) and fisher. The same colour gradient is applied to all maps within individual case studies to emphasise differences in intensity. (D) For each case study, the relative differences in minimum core area containing 50% of predicted use for SSD versus RSF, SSF, and ABM predictions (e.g., RSF-SSD/RSF) are plotted for individuals. For visualisation, the mean and range of these relative differences are overlaid on individual estimates. All organism silhouettes are from PhyloPic (www.phylopic.org).

novel contexts. Similarly, naïve SSF predictions, which ignore cumulative movement constraints, performed even worse than RSFs, consistent with previous work showing that habitat selection kernels from iSSFs alone poorly predict emergent space use (Barnett and Moorcroft 2008; Avgar et al. 2016; Signer et al. 2017; Michelot et al. 2019). By integrating both local habitat selection and movement, SSD consistently captured emergent space use patterns and generalised better to out-of-sample conditions than either RSF or naïve SSF approaches. Moreover, SSD closely matched or outperformed ABMs despite requiring orders of magnitude lower computational resources than ABMs. As evidence of our framework's utility, SSD predictions were able to scale movements from six individual buffalo to better capture nearly three decades of population-level densities across Kruger National Park, outperforming all alternative approaches. Together, these results demonstrate that individual-level movement data—a rapidly expanding resource for biodiversity monitoring (Jetz et al. 2022; Kays and Wikelski 2023; Davidson et al. 2025)—can be leveraged through SSD to efficiently link individual movement mechanisms to population-level spatial distributions.

The SSD framework advances prior work in mechanistic space use modelling by providing a practical, computationally efficient approach to predict emergent space use from movement data. Our framework treats local movement as a Markovian process and solves for steady-state distributions, following approaches in spatial ecology (Fletcher Jr. et al. 2019). By applying our framework to scale local habitat selection and movement processes, we innovate on prior approaches in two key ways. First, we formally link iSSF estimates to local movement probabilities. Though work in connectivity science has used movement models to parametrise transition matrices, these approaches map relative selection strengths from iSSFs (either based on global or semi-local comparisons) and transform maps into resistance layers (Zeller et al. 2012, 2016; Keeley et al. 2016; Panzacchi et al. 2016). Instead, we directly estimate movement rates between cells from the iSSF, inclusive of empirical habitat selection patterns and movement constraints. We achieve this by kernelising the relative selection strength of discrete movement choices, resulting in directional movement probabilities without relying on post hoc transformations. Our second innovation addresses the long-standing computational challenges of solving large transition matrices (see Appendix E of Potts and Borger 2023). By leveraging the inherently local nature of animal movement—where more distant movements become increasingly improbable—SSD treats transition matrices as sparse, drastically reducing computational costs without sacrificing accuracy. In contrast to agent-based

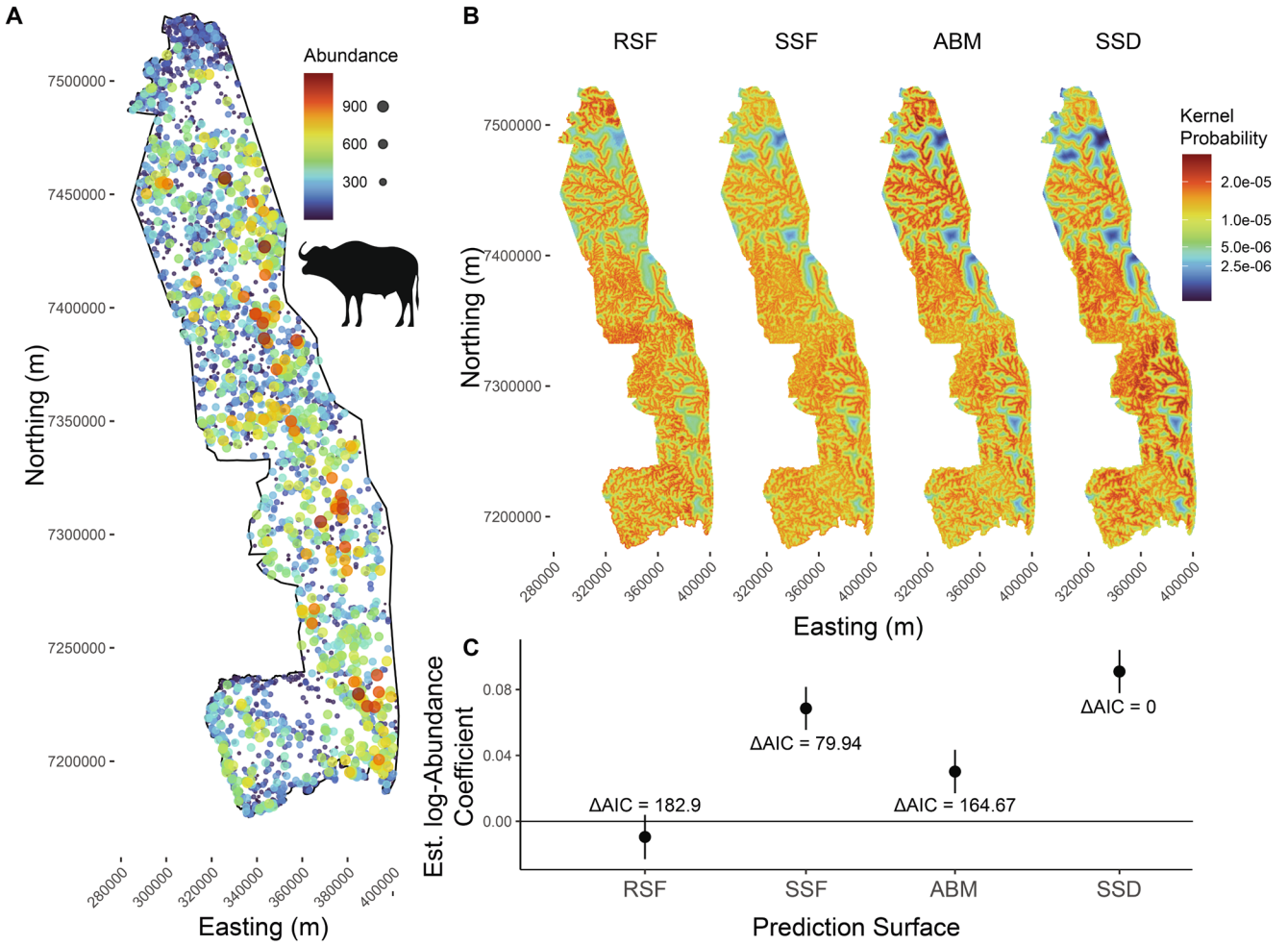

FIGURE 6 | Individual-level movement models capture emergent population density. (A) Dry-season helicopter census data for mixed African buffalo herds in Kruger National Park, South Africa (outline). Point size and colour correspond to observed herd size. (B) Average space use predictions from resource selection functions (RSFs), naïve step-selection functions (SSFs), agent-based model simulations (ABMs) and stable state distributions (SSDs). The same colour gradient is applied to all maps to emphasise differences in intensity. (C) Coefficients for a 1-standard deviation change in predicted space use kernel surfaces relative to abundance from negative binomial mixed-effect models, with AIC comparison of model fits. Points and ranges denote estimates and 95% CIs. The African buffalo silhouette is from PhyloPic (www.phylopic.org).

models (ABMs), which require extensive forward simulation to approximate stable space use and are not guaranteed to converge (Signer et al. 2017, 2024; Michelot et al. 2019; Potts and Borger 2023; Forrest et al. 2024), SSD directly solves for long-term space use via eigendecomposition. We found that sparse matrices enable SSD to scale efficiently to large landscapes, producing predictions in minutes on standard hardware (16 GB RAM). Together, these innovations position SSD as a scalable alternative to ABMs, achieving equivalent or superior predictions with orders of magnitude lower computational effort.

While SSD offers major advantages, there are contexts where ABMs may be preferable. In simulations, ABMs slightly outperformed SSD in heterogeneous landscapes under strong selection pressures, likely by incorporating finer-scale movement processes such as directional persistence or by operating in continuous space. Though ABMs and SSD should theoretically converge to the same solution, there were instances, like in the roe deer example, where ABMs and SSD were dissimilar. This discordance could be a result of high inter-individual variation in habitat selection (S2 Figure S8), resulting in predictive differences at the scale of individuals (Figure 4B) or potentially because ABMs capture longer, directional movements that generate more dispersive space use than SSD (S2 Figure S11, Figure 5B). Interestingly, ABMs also generally produced more accurate predictions in the fisher system, which had the most resolute GPS tracking of all empirical examples (30 min). Potentially, ABMs are more advantageous when fine-scale movement behaviours besides step lengths are expected to shape emergent space use. SSD also treats environments and movement as static processes, limiting its applicability when dynamic behavioural regimes or environments strongly affect space use (e.g., Forrest et al. 2024).

Our findings position the SSD framework as a practical, scalable tool for predicting animal space use from individual movement data. By explicitly integrating habitat preferences and movement constraints, SSD bridges a persistent gap between movement models and broad-scale spatial predictions. Notably, SSD successfully scaled from individual GPS tracks to predict long-term population densities in a large, real-world system. This underscores the potential for SSD in ecological modelling and conservation planning, particularly if predictions of empirical

density are replicated in other systems. Additionally, assessing mechanistic movement model fit remains challenging, often relying on step-level diagnostics of movement or habitat use (Fieberg et al. 2018, 2024; Signer et al. 2024). However, discrepancies between local movement processes and emergent space use can be difficult to detect (Michelot et al. 2019; Fieberg et al. 2024). By comparing SSD-predicted space use to observed or expected distributions, researchers can evaluate whether fitted movement models produce realistic spatial patterns, offering a scalable tool for diagnosing overfitting, missing covariates, or structural misspecification. Finally, we found that SSD tended to perform better on challenging out-of-sample predictions than other frameworks. Future work should investigate how hierarchical movement modelling across individuals, populations, and geographic distributions (e.g., Muff et al. 2019; Chatterjee et al. 2024; Klappstein et al. 2024) could further increase the predictive performance of SSD across inferential scales.

Author Contributions

W.R. and S.Y. conceptualised the paper. W.R. wrote the code and carried out the analyses supporting the manuscript. W.R. wrote the initial draft with contributions from S.Y. All authors provided feedback on the concept and contributed to the final draft.

Acknowledgements

We thank Johannes Signer, Francesca Cagnacci, Scott LaPoint, and Paul Cross for their generosity in providing the red deer, roe deer, fisher, and buffalo datasets (respectively) as open-access resources for the scientific community, and we thank SANParks for providing the buffalo census data. We also thank the Yale Center for Research Computing, which was used to run simulations. We also thank John Fieberg for initial discussion and members of the Jetz and Ezenwa labs for their feedback. We greatly appreciate editor and reviewer feedback, which substantially improved the manuscript. W.R. received funding from the Gruber Foundation. S.Y. received funding from the Max Planck–Yale Center for Biodiversity Movement and Global Change.

Data Availability Statement

South African National Parks (SANParks) provided Kruger National Park African buffalo census data and spatial data layers. All other data used were simulated or open source, and movement data were used with expressed approval by the original authors. Code to replicate results, buffalo census data, and spatial data are available at https://github.com/will-rogers/SSD_Paper_Code and archived on Zenodo: https://doi.org/10.5281/zenodo.16794098.

Peer Review

The peer review history for this article is available at https://www.webofscience.com/api/gateway/wos/peer-review/10.1111/ele.70279.

References

Aarts, G., J. Fieberg, and J. Matthiopoulos. 2012. "Comparative Interpretation of Count, Presence–Absence and Point Methods for Species Distribution Models." *Methods in Ecology and Evolution* 3: 177–187.

Akaike, H. 1998. "Information Theory and an Extension of the Maximum Likelihood Principle." In *Selected Papers of Hirotugu Akaike*, 199–213. Springer.

Alston, J. M., C. H. Fleming, R. Kays, et al. 2023. "Mitigating Pseudoreplication and Bias in Resource Selection Functions With Autocorrelation-Informed Weighting." *Methods in Ecology and Evolution* 14: 643–654.

Andrén, H. 1994. "Effects of Habitat Fragmentation on Birds and Mammals in Landscapes With Different Proportions of Suitable Habitat: A Review." *Oikos* 71: 355–366.

Avgar, T., S. R. Lele, J. L. Keim, and M. S. Boyce. 2017. "Relative Selection Strength: Quantifying Effect Size in Habitat- and Step-Selection Inference." *Ecology and Evolution* 7: 5322–5330.

Avgar, T., J. R. Potts, M. A. Lewis, and M. S. Boyce. 2016. "Integrated Step Selection Analysis: Bridging the Gap Between Resource Selection and Animal Movement." *Methods in Ecology and Evolution* 7: 619–630.

Barnett, A. H., and P. R. Moorcroft. 2008. "Analytic Steady-State Space Use Patterns and Rapid Computations in Mechanistic Home Range Analysis." *Journal of Mathematical Biology* 57: 139–159.

Barve, N., V. Barve, A. Jiménez-Valverde, et al. 2011. "The Crucial Role of the Accessible Area in Ecological Niche Modeling and Species Distribution Modeling." *Ecological Modelling* 222: 1810–1819.

Boyce, M. S., and L. L. McDonald. 1999. "Relating Populations to Habitats Using Resource Selection Functions." *Trends in Ecology & Evolution* 14: 268–272.

Boyce, M. S., P. R. Vernier, S. E. Nielsen, and F. K. A. Schmiegelow. 2002. "Evaluating Resource Selection Functions." *Ecological Modelling* 157: 281–300.

Brooks, M. E., K. Kristensen, K. J. Van Benthem, et al. 2017. "glmmTMB Balances Speed and Flexibility Among Packages for Zero-Inflated Generalized Linear Mixed Modeling." *R Journal* 9: 378–400.

Cagnacci, F., S. Focardi, M. Heurich, et al. 2011. "Partial Migration in Roe Deer: Migratory and Resident Tactics Are End Points of a Behavioural Gradient Determined by Ecological Factors." *Oikos* 120: 1790–1802.

Chatterjee, N., D. Wolfson, D. Kim, et al. 2024. "Modelling Individual Variability in Habitat Selection and Movement Using Integrated Step-Selection Analysis." *Methods in Ecology and Evolution* 15: 1034–1047.

Cross, P. C., J. A. Bowers, C. T. Hay, et al. 2016. *Data From: Nonparameteric Kernel Methods for Constructing Home Ranges and Utilization Distributions*. Movebank Data Repository.

Davidson, S. C., F. Cagnacci, P. Newman, et al. 2025. "Establishing Bio-Logging Data Collections as Dynamic Archives of Animal Life on Earth." *Nature Ecology & Evolution* 9: 204–213.

Elith, J., and J. R. Leathwick. 2009. "Species Distribution Models: Ecological Explanation and Prediction Across Space and Time." *Annual Review of Ecology, Evolution, and Systematics* 40: 677–697.

Elith, J., S. J. Phillips, T. Hastie, M. Dudík, Y. E. Chee, and C. J. Yates. 2011. "A Statistical Explanation of MaxEnt for Ecologists." *Diversity and Distributions* 17: 43–57.

Fieberg, J. R., J. D. Forester, G. M. Street, D. H. Johnson, A. A. ArchMiller, and J. Matthiopoulos. 2018. "Used-Habitat Calibration Plots: A New Procedure for Validating Species Distribution, Resource Selection, and Step-Selection Models." *Ecography* 41: 737–752.

Fieberg, J., S. Freeman, and J. Signer. 2024. "Using Lineups to Evaluate Goodness of Fit of Animal Movement Models." *Methods in Ecology and Evolution* 15: 1048–1059.

Fieberg, J., J. Signer, B. Smith, and T. Avgar. 2021. "A 'How to' Guide for Interpreting Parameters in Habitat-Selection Analyses." *Journal of Animal Ecology* 90: 1027–1043.

Fletcher, R. J., Jr., J. A. Sefair, C. Wang, et al. 2019. "Towards a Unified Framework for Connectivity That Disentangles Movement and Mortality in Space and Time." *Ecology Letters* 22: 1680–1689.

Forrest, S. W., D. Pagendam, M. Bode, et al. 2024. "Predicting Fine-Scale Distributions and Emergent Spatiotemporal Patterns From Temporally Dynamic Step Selection Simulations." *Ecography* 2025: e07421.

Gomez, S., H. M. English, V. Bejarano Alegre, et al. 2025. "Understanding and Predicting Animal Movements and Distributions in the Anthropocene." *Journal of Animal Ecology* 94: 1146–1164.

Hanson, J. O., R. Schuster, M. Strimas-Mackey, et al. 2024. "Systematic Conservation Prioritization With the Prioritizr R Package." *Conservation Biology* 39: e14376.

Hartig, F. 2018. "DHARMa: Residual Diagnostics for Hierarchical (Multi-Level/Mixed) Regression Models." R Packag Version 020.

Hooten, M. B., D. S. Johnson, B. T. McClintock, and J. M. Morales. 2017. *Animal Movement: Statistical Models for Telemetry Data*. CRC Press.

Hughes, K., G. T. Fosgate, C. M. Budke, M. P. Ward, R. Kerry, and B. Ingram. 2017. "Modeling the Spatial Distribution of African Buffalo (*Syncerus caffer*) in the Kruger National Park, South Africa." *PLoS One* 12: e0182903.

James, F. C., R. F. Johnston, N. O. Wamer, G. J. Niemi, and W. J. Boecklen. 1984. "The Grinnellian Niche of the Wood Thrush." *American Naturalist* 124: 17–47.

Jetz, W., G. Tertitski, R. Kays, et al. 2022. "Biological Earth Observation With Animal Sensors." *Trends in Ecology & Evolution* 37: 293–298.

Johnson, D. S., M. B. Hooten, and C. E. Kuhn. 2013. "Estimating Animal Resource Selection From Telemetry Data Using Point Process Models." *Journal of Animal Ecology* 82: 1155–1164.

Kays, R., and M. Wikelski. 2023. "The Internet of Animals: What It Is, What It Could Be." *Trends in Ecology & Evolution* 38: 859–869.

Keeley, A. T. H., P. Beier, and J. W. Gagnon. 2016. "Estimating Landscape Resistance From Habitat Suitability: Effects of Data Source and Nonlinearities." *Landscape Ecology* 31: 2151–2162.

Klappstein, N. J., T. Michelot, J. Fieberg, E. J. Pedersen, and J. Mills Flemming. 2024. "Step Selection Functions With Non-Linear and Random Effects." *Methods in Ecology and Evolution* 15: 1332–1346.

LaPoint, S., P. Gallery, M. Wikelski, and R. Kays. 2013. "Animal Behavior, Cost-Based Corridor Models, and Real Corridors." *Landscape Ecology* 28: 1615–1630.

Leslie, P. H. 1945. "On the Use of Matrices in Certain Population Mathematics." *Biometrika* 33: 183–212.

MacKenzie, D., J. Nichols, J. A. Royle, K. Pollock, L. Bailey, and J. Hines. 2006. *Occupancy Estimation and Modeling: Inferring Patterns and Dynamics of Species Occurrence*. Elsevier.

Matthiopoulos, J., J. Fieberg, G. Aarts, F. Barraquand, and B. E. Kendall. 2020. "Within Reach? Habitat Availability as a Function of Individual Mobility and Spatial Structuring." *American Naturalist* 195: 1009–1026.

McRae, B. H., B. G. Dickson, T. H. Keitt, and V. B. Shah. 2008. "Using Circuit Theory to Model Connectivity in Ecology, Evolution, and Conservation." *Ecology* 89: 2712–2724.

Merow, C., M. J. Smith, T. C. Edwards Jr., et al. 2014. "What Do We Gain From Simplicity Versus Complexity in Species Distribution Models?" *Ecography* 37: 1267–1281.

Michelot, T., P. G. Blackwell, and J. Matthiopoulos. 2019. "Linking Resource Selection and Step Selection Models for Habitat Preferences in Animals." *Ecology* 100: e02452.

Muff, S., J. Signer, and J. Fieberg. 2019. "Accounting for Individual-Specific Variation in Habitat-Selection Studies: Efficient Estimation of Mixed-Effects Models Using Bayesian or Frequentist Computation." *Journal of Animal Ecology* 89: 80–92.

Munguía, M., A. Townsend Peterson, and V. Sánchez-Cordero. 2008. "Dispersal Limitation and Geographical Distributions of Mammal Species." *Journal of Biogeography* 35: 1879–1887.

Nathan, R., W. M. Getz, E. Revilla, et al. 2008. "A Movement Ecology Paradigm for Unifying Organismal Movement Research." *Proceedings of the National Academy of Sciences of the United States of America* 105: 19052–19059.

Panzacchi, M., B. Van Moorter, O. Strand, et al. 2016. "Predicting the Continuum Between Corridors and Barriers to Animal Movements Using Step Selection Functions and Randomized Shortest Paths." *Journal of Animal Ecology* 85: 32–42.

Pearson, R. G., and T. P. Dawson. 2003. "Predicting the Impacts of Climate Change on the Distribution of Species: Are Bioclimate Envelope Models Useful?" *Global Ecology and Biogeography* 12: 361–371.

Potts, J. R., G. Bastille-Rousseau, D. L. Murray, J. A. Schaefer, and M. A. Lewis. 2014. "Predicting Local and Non-Local Effects of Resources on Animal Space Use Using a Mechanistic Step Selection Model." *Methods in Ecology and Evolution* 5: 253–262.

Potts, J. R., and L. Borger. 2023. "How to Scale Up From Animal Movement Decisions to Spatiotemporal Patterns: An Approach via Step Selection." *Journal of Animal Ecology* 92: 16–29.

Pulliam, H. R. 2000. "On the Relationship Between Niche and Distribution." *Ecology Letters* 3: 349–361.

Qiu, Y., and M. Jiali. 2024. "RSpectra: Solvers for Large-Scale Eigenvalue and SVD Problems."

Rogers, W., S. Yanco, and W. Jetz. 2025. "Data and Code to Support: 'Choices to Landscapes: Mechanisms of Animal Movement Scale to Landscape Patterns of Space Use'." Zenodo.

Schick, R. S., S. R. Loarie, F. Colchero, et al. 2008. "Understanding Movement Data and Movement Processes: Current and Emerging Directions." *Ecology Letters* 11: 1338–1350.

Signer, J., J. Fieberg, and T. Avgar. 2017. "Estimating Utilization Distributions From Fitted Step-Selection Functions." *Ecosphere* 8: e01771.

Signer, J., J. Fieberg, and T. Avgar. 2019. "Animal Movement Tools (Amt): R Package for Managing Tracking Data and Conducting Habitat Selection Analyses." *Ecology and Evolution* 9: 880–890.

Signer, J., J. Fieberg, B. Reineking, et al. 2024. "Simulating Animal Space Use From Fitted Integrated Step-Selection Functions (iSSF)." *Methods in Ecology and Evolution* 15: 43–50.

Soberón, J. 2007. "Grinnellian and Eltonian Niches and Geographic Distributions of Species." *Ecology Letters* 10: 1115–1123.

Soberón, J., and A. T. Peterson. 2005. "Interpretation of Models of Fundamental Ecological Niches and Species' Distributional Areas." *Biodiversity Informatics* 2: 1–10.

Staver, A. C., C. Wigley-Coetsee, and J. Botha. 2019. "Grazer Movements Exacerbate Grass Declines During Drought in an African Savanna." *Journal of Ecology* 107: 1482–1491.

Urban, M., K. Heckel, C. Berger, et al. 2020. "Woody Cover Mapping in the Savanna Ecosystem of the Kruger National Park Using Sentinel-1 C-Band Time Series Data." *KOEDOE—African Protected Area Conservation and Science* 62: a1621.

Van Moorter, B., I. Kivimaki, M. Panzacchi, et al. 2023. "Habitat Functionality: Integrating Environmental and Geographic Space in Niche Modeling for Conservation Planning." *Ecology* 104: e4105.

Zeller, K. A., K. McGarigal, S. A. Cushman, P. Beier, T. W. Vickers, and W. M. Boyce. 2016. "Using Step and Path Selection Functions for Estimating Resistance to Movement: Pumas as a Case Study." *Landscape Ecology* 31: 1319–1335.

Zeller, K. A., K. McGarigal, and A. R. Whiteley. 2012. "Estimating Landscape Resistance to Movement: A Review." *Landscape Ecology* 27: 777–797.

Supporting Information

Additional supporting information can be found online in the Supporting Information section. **Data S1 and S2:** ele70279-sup-0001-supinfo.docx.